Supporting Information

Strong-Weak Binary Solvation Structure for Unimpeded Low-Temperature Ion Transport in Nanoporous Energy Storage Materials

Huachao Yang[a,b], Zifan Wang[a], Yiheng Qi[a], Qinghu Pan[a], Chuanzhi Zhang[a], Yuhui Huang[b,c], Jianhua Yan[a], Kefa Cen[a], Guoping Xiong[d], Zheng Bo*[a], and Kostya (Ken) Ostrikov[e]

[a.] State Key Laboratory of Clean Energy Utilization, College of Energy Engineering, Zhejiang University, Hangzhou, Zhejiang, 310027, China

E-mail: bozh@zju.edu.cn

[b.] Research Institute of Zhejiang University-Taizhou, Taizhou, Zhejiang, 318000, China

[c.] College of Materials Science and Engineering, Zhejiang University, Hangzhou, Zhejiang, 310027, China

[d.] Department of Mechanical Engineering, The University of Texas at Dallas, Richardson, Texas, TX 75080, United States

[e.] School of Chemistry and Physics and QUT Centre for Materials Science, Queensland University of Technology (QUT), Brisbane, QLD 4000, Australia

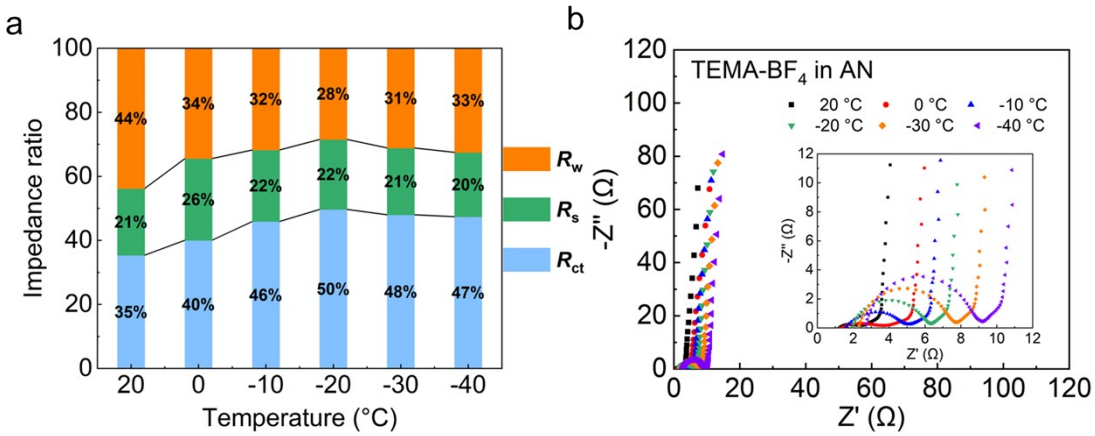

Figure S1. (a) Impedance ratio of R_s, R_{ct}, R_w in AN-based electrolyte under different temperatures. (b) Nyquist plots of AN-based electrolyte coin cell supercapacitors at different temperatures.

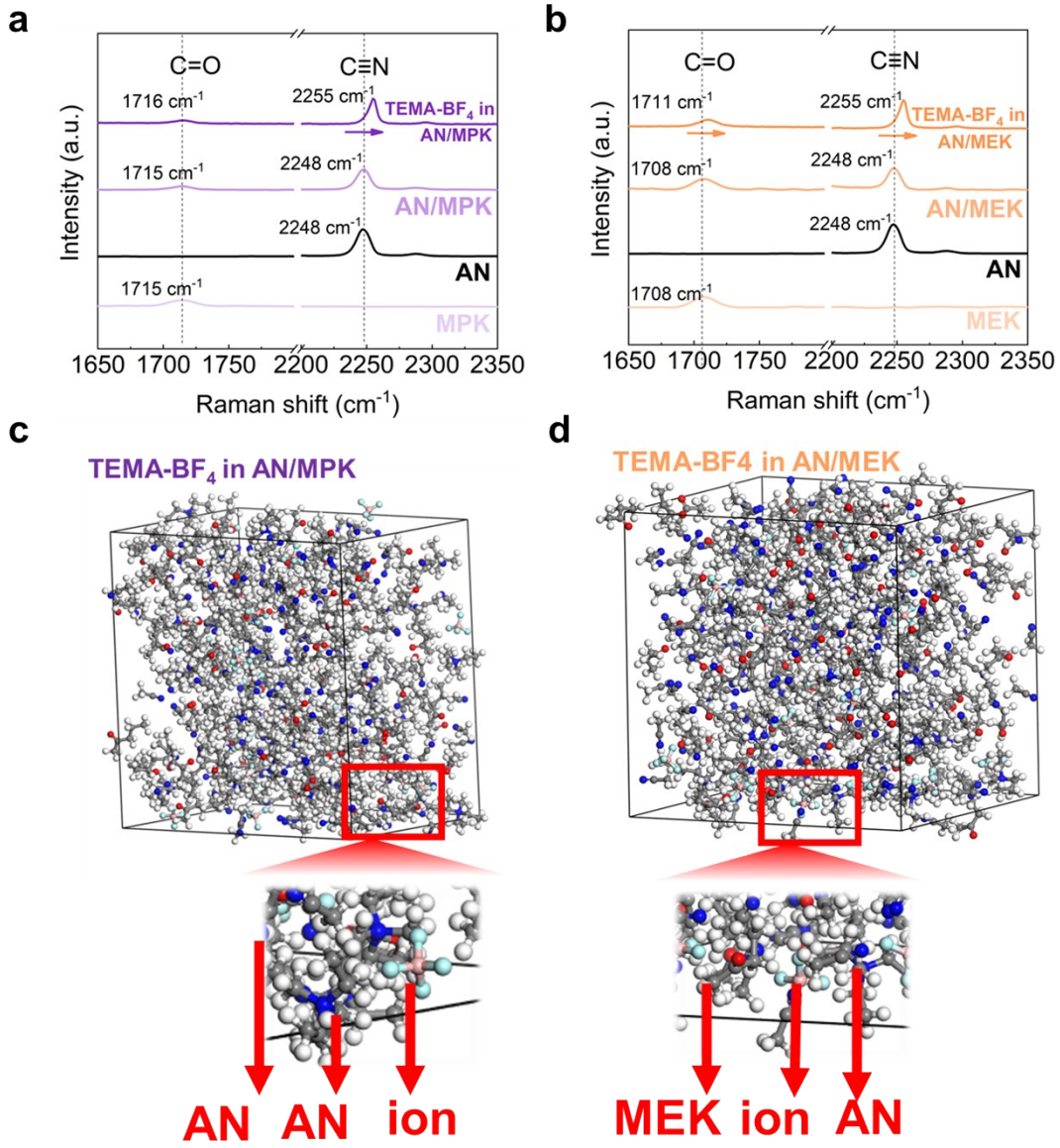

Figure S2. (a–b) Raman spectroscopy of single solvent (MPK, MEK, AN solvent), solvent mixtures (AN/MPK, AN/MEK), and electrolytes (TEMA-BF_4 in AN/MPK, AN/MEK). (c–d) Snapshots of molecular dynamics simulations. (Atom Colors: B, pink; C, grey; F, light blue; H, white; N, dark blue; O, red.)

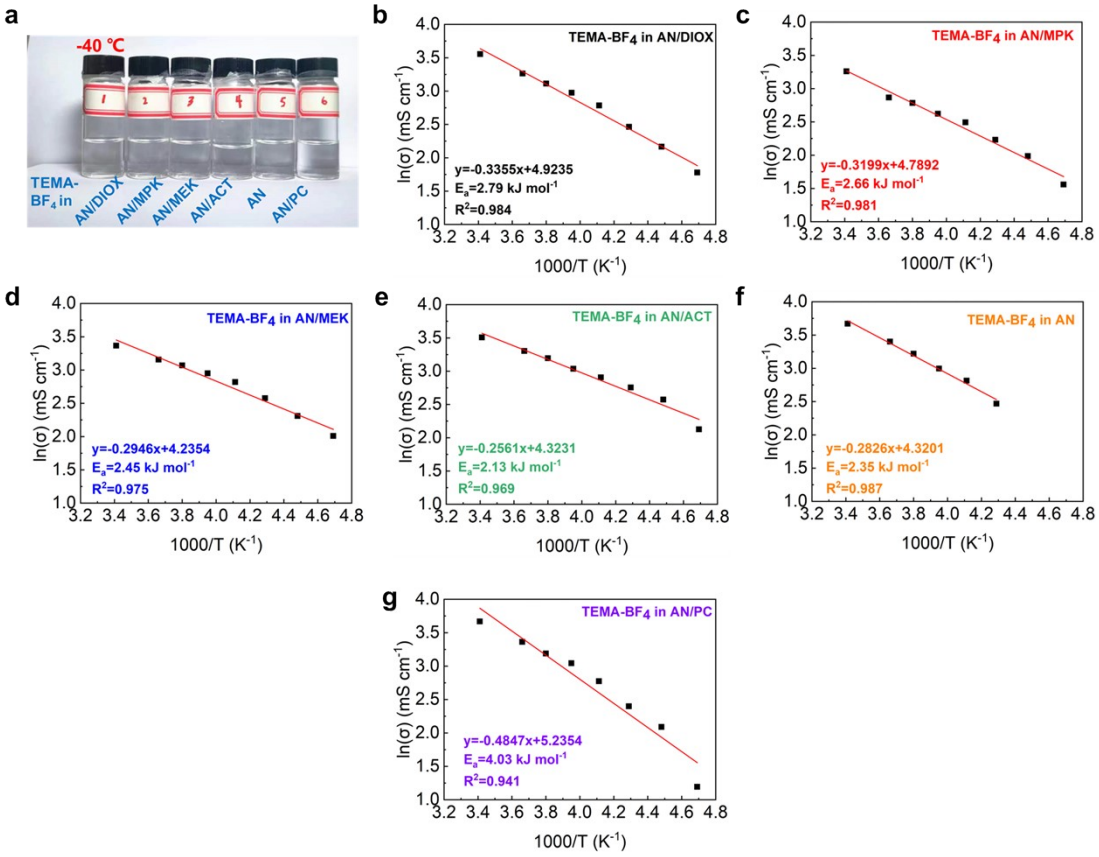

Figure S3. (a) Freezing tests of different electrolytes at −40 °C. (b-g) Arrhenius plots of ionic conductivities of electrolytes.

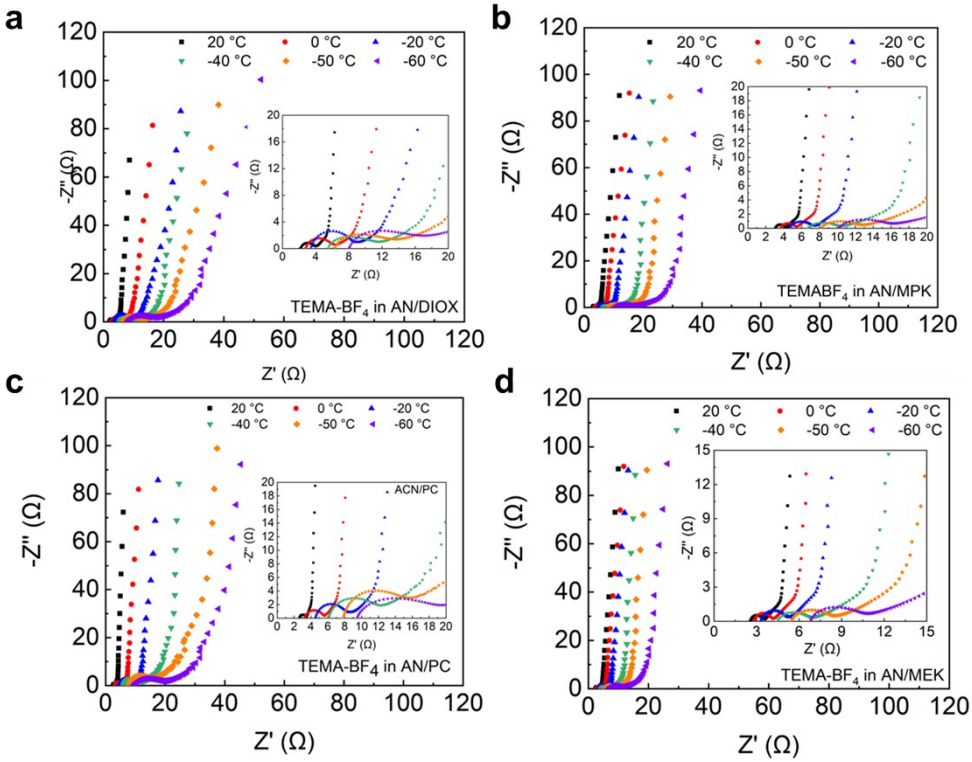

Figure S4. (a−d) Nyquist plots of different electrolytes based coin cell supercapacitors at different temperatures.

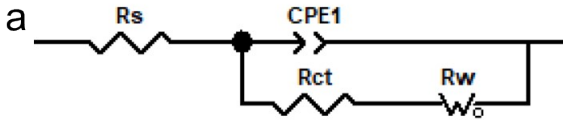

Figure S5. The corresponding equivalent circuit diagram of TEMA-BF_4 in AN/X-based coin cell supercapacitor. Here, X stands for DIOX, MPK, MEK, ACT and PC.

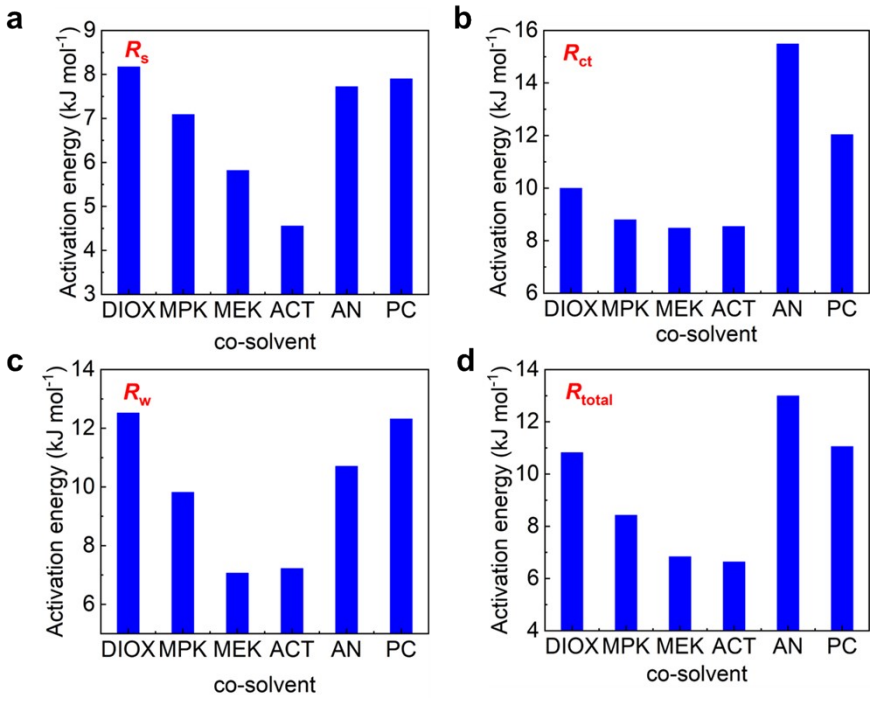

Figure S6. Activation energies of impedance in different co-solvent-based electrolytes. The activation energies of (a) R_s, (b) R_{ct}, (c) R_w and (d) R in DIOX/MPK/MEK/ACT/PC co-solvent-based electrolytes.

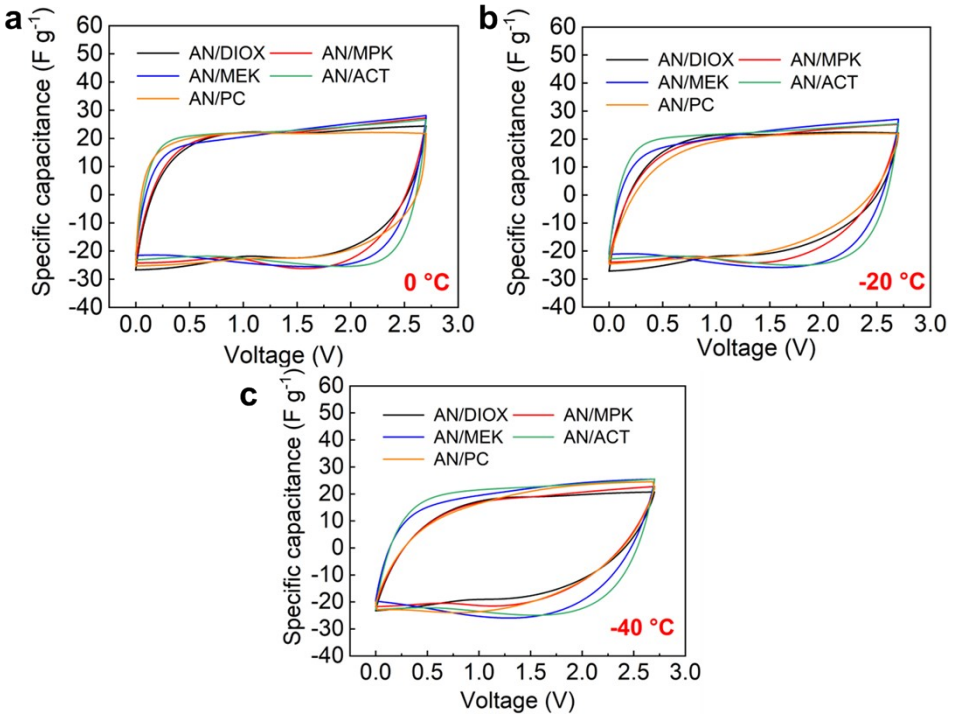

Figure S7. Cyclic voltammetry plots of different electrolytes based coin cell supercapacitors at different temperatures.

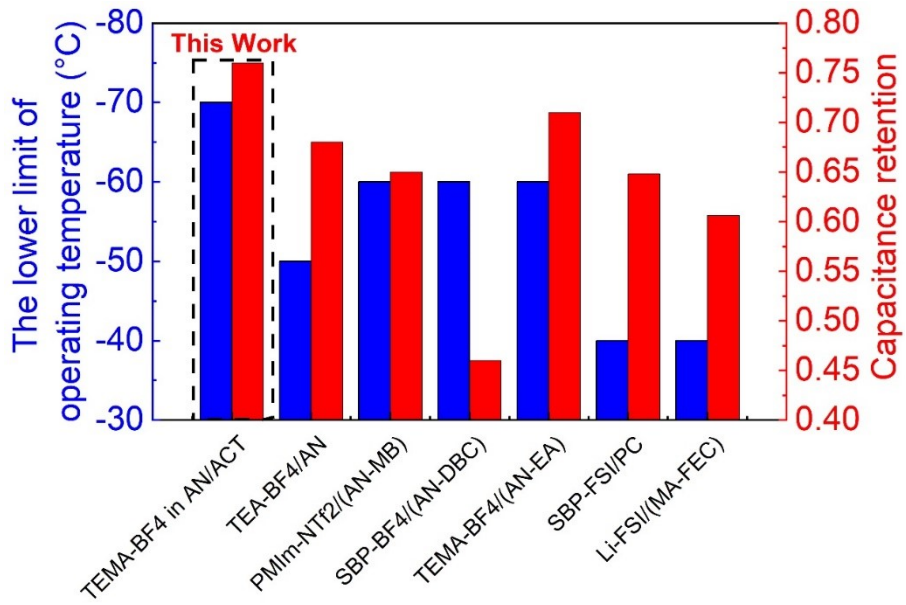

Figure S8. The lower limit of operating temperature and corresponding capacitance retention rate of TEMA-BF_4 in AN/ACT, TEA-BF_4/AN, PMIm-NTf_2/(AN-MB)[1], SBP-BF_4/(AN-DBC)[2], TEMA-BF_4/(AN-EA)[3], SBP-FSI/PC[4], Li-FSI/(MA-FEC)[5] electrolytes.

Table S1. Comparison of binding energy obtained from DFT calculation.

Systems	Total	Cation	Anion	E_b (Ha)	E_b (eV)
$TEMABF_4$	−757.63	−332.96	−424.60	−0.060717	−1.65
$TEMABF_4$ -AN	−890.62	−332.96	−557.60	−0.051869	−1.41
$TEMABF_4$ -AN-ACT	−1084.10	−332.96	−751.09	−0.043255	−1.17
$TEMABF_4$-AN-AN	−1123.47	−332.96	−790.46	−0.043927	−1.23
$TEMABF_4$-AN-PC	−1272.90	−332.96	−939.89	−0.045937	−1.25

References

[1] X. Tang, D. Xiao, Z. Xu, Q. Liu, B. Ding, H. Dou, X. Zhang, *J. Mater. Chem. A* **2022**, *10*, 18374–18382;

[2] F. Cheng, X. Yu, J. Wang, Z. Shi, C. Wu, *Electrochimica Acta* **2016**, *200*, 106–114;

[3] R. R. Galimzyanov, S. V. Stakhanova, I. S. Krechetov, A. T. Kalashnik, M. V. Astakhov, A. V. Lisitsin, A. Y. Rychagov, T. R. Galimzyanov, F. S. Tabarov, *J. Power Sources* **2021**, *495*, 229442;

[4] W. Zhang, J. Wang, D. Ruan, Q. Shi, F. Zhang, Q. Ren, Z. Shi, *Chem. Eng. J.* **2019**, *373*,1012-1019

[5] X. Meng, J. Qin, Y. Liu, Z. Liu, Y. Zhao, Z. Song, H. Zhan, *Chem. Eng. J.* **2023**, *465*, 142913.